GSI Annual Report 2007 (extracts)

Chemistry

TASCA

First successful chemistry-experiment behind TASCA - Electrodeposition of Os ***Page 4***
J. Even, W. Brüchle, R. A. Buda, C. E. Düllmann, K. Eberhardt, E. Jäger, H. Jungclas, J. V. Kratz, J. Khuyagbaatar, D. Liebe, M. Mendel, M. Schädel, B. Schausten, E. Schimpf, A. Semchenkov, A. Türler, V. Vicente Vilas, N. Wiehl, T. Wunderlich, A. Yakushev

Theory

The new Isotope ^{271}Hs Observed in the ^{26}Mg(^{248}Cm,3n) Reaction

J. Dvorak[1], Z. Dvorakova[1], R. Krücken[1], F. Nebel[1], R. Perego[1], R. Schuber[1], A. Semchenkov[1, 2], A. Türler[1], B. Wierczinski[1], A. Yakushev[1], W. Brüchle[2], Ch. E. Düllmann[2, 3, 4], E. Jäger[2], M. Schädel[2], B. Schausten[2], E. Schimpf[2], M. Chelnokov[5], V. Gorshkov[5], A. Kuznetsov[5], A. Yeremin[5], K. Eberhardt[6], P. Thörle[6], Y. Nagame[7], K. Nishio[7], Z. Qin[2, 8], and M. Wegrzecki[9]

[1]TU Munich, Garching, Germany; [2]GSI, Darmstadt, Germany; [3]LBNL, Berkeley, CA, USA; [4]UC, Berkeley, CA, USA; [5]JINR, Dubna, Russia; [6]U Mainz, Germany; [7]JAEA, Tokai-mura, Japan; [8]IMP, Lanzhou, China; [9]ITE, Warsaw, Poland

Heavy-ion hot-fusion reactions with actinide targets have been extensively used to produce relatively neutron-rich superheavy elements (SHE), i.e. elements with atomic numbers $Z \geq 104$. In these reactions surviving SHE nuclei are usually formed after evaporation of four or more neutrons. Consequently, up to now only 4*n* and 5*n* evaporation channels have been exploited in the synthesis of SHE with beams up to $Z = 16$. Lower x*n* channels were not studied, probably due to the fact that the magnitude of the 3*n* channel was decreasing rapidly in the sequence of carbon, nitrogen, and oxygen induced reactions. This has commonly been interpreted as the vanishing of the 3*n* channel with increasing atomic number of the projectile. In this work, we report the successful search for the 3*n* evaporation channel product of the hot fusion reaction ^{26}Mg + ^{248}Cm the new isotope ^{271}Hs.

Hassium nuclei were produced in the reaction ^{248}Cm(^{26}Mg, x*n*)$^{274-x}$Hs at the UNILAC at GSI and isolated using the efficient on-line chemical separation and detection system COMPACT [1]. In two runs Hs isotopes were produced at 5 different beam energies from 130 to 150 MeV in the centre of the target (see Table 1). In the first run [1], the unique chain No. 14 observed at a beam energy of 136 MeV could be attributed neither to the decay of ^{269}Hs nor to ^{270}Hs. The first α-particle had an energy of 9.30 MeV, followed after 149.2 s by an α-particle with an energy of 8.20 MeV. The chain was terminated by fission after another 12 s. It was proposed that this decay chain originates from the decay of ^{271}Hs. In the second run we observed four more chains at beam energies of 130 MeV (3 events) and 140 MeV (1 event) with unique decay properties different from ^{269,270}Hs.

Table 1. Decay chains of ^{271}Hs observed in this work at beam energy E_{Lab}. In detector numbers, #, , t stands for "top detector" and b for "bottom detector".

E_{Lab}, (MeV)	$E_{\alpha 1}$,(^{271}Hs) (MeV) (#)	Δt_1, (s)	$E_{\alpha 2/SF}$,(^{267}Sg) (MeV) (#)	Δt_2, (s)	E_{SF},(^{263}Rf) (MeV) (#)
130	9.16(24t)	142	26/--(25b/--)		
130	9.02(16b)	30.4	89/68(15t/15b)		
130	9.23(20t)	264	15/83(20t/19b)		
136*	9.30(7t)	149	8.20(7t)	12	89/95(7t/7b)
136*	9.10(14t)	96	80/90(14t/13b)		
140	9.14(12t)	47.9	69/--(12t/--)		

* events from [2], see text for details.

* Work supported by BMBF (06MT247I)

All these additional events are characterized by a first α-particle with an energy > 9 MeV and were terminated by SF with long lifetimes. Three of these chains were detected at 130 MeV beam energy. This is below the expected maximum of the 4*n* channel and far below the energy where significant contribution of the 5n channel is expected. The decay chain No. 10 in [2] was tentatively attributed to the decay of ^{269}Hs, assuming that the α-particle from the decay of ^{265}Sg is missing. This α-SF chain was detected at 136 MeV beam energy, about 10 MeV below the maximum of the 5*n* channel. The α-particle energy was 9.10 MeV and SF followed after 96 s, similar to chains observed in the second run mostly at 130 MeV. It is very unlikely (0.03%) to always miss the second α-particle (Sg decay) in five decay chains observed at lower beam energies. Therefore, all these six chains were attributed to the new isotope ^{271}Hs produced in the 3*n* evaporation channel. Taking into account the long α-decay life-time for ^{267}Sg detected in the chain mentioned before, which is consistent with the relatively low energy of the detected α-particle, partial SF and α-decay half-lives may become sufficiently similar that branching into both decay modes can be observed.

In total we have observed 26 nuclear decay chains from Hs isotopes assigned to ^{269}Hs (5*n*), ^{270}Hs (4*n*), and ^{271}Hs (3*n*) with the decay properties summarized in Table 2. The measured cross section for the 3*n* channel is unexpectedly high, similar to that of the 4*n* and 5*n* channels [2]. This is in strong contrast to expectations based on the idea of a "vanishing" 3*n* channel in hot fusion reactions with increasing projectile atomic number.

Table 2. Decay properties of Hs isotopes.

Nuclei	Half-life	E_α, (MeV)[#]
^{269}Hs	--	8.95 ± 0.05
	4 s[†]	9.13 ± 0.05
^{270}Hs	23 s[†]	8.88 ± 0.05
^{271}Hs	4 s[†]	9.13 ± 0.05
	--	9.30 ± 0.05

[#]Most probable energy considering the peak shape as measured in a calibration run.

[†]Half-life calculated from E_α values of the most probable transitions using the formalism of Ref. [3].

References

[1] J. Dvorak *et al*., Phys. Rev. Lett. **97**, 242501 (2006).
[2] J. Dvorak *et al*., GSI Sci. Rep. 2007, this issue.
[3] A. Parkhomenko and A. Sobiczewski, Acta Phys. Pol. B **36**, 3095 (2005).

Cross Section Measurements of the Reaction ^{26}Mg(^{248}Cm,xn) $^{274-x}$Hs*

J. Dvorak[1], Z. Dvorakova[1], R. Krücken[1], F. Nebel[1], R. Perego[1], R. Schuber[1], A. Semchenkov[1, 2], A. Türler[1], B. Wierczinski[1], A. Yakushev[1], W. Brüchle[2], Ch. E. Düllmann[2, 3, 4], E. Jäger[2], M. Schädel[2], B. Schausten[2], E. Schimpf[2], M. Chelnokov[5], V. Gorshkov[5], A. Kuznetsov[5], A. Yeremin[5], K. Eberhardt[6], P. Thörle[6], Y. Nagame[7], K. Nishio[7], Z. Qin[2, 8], and M. Wegrzecki[9]

[1]TU Munich, Garching, Germany; [2]GSI, Darmstadt, Germany; [3]LBNL, Berkeley, CA, USA; [4]UC, Berkeley, CA, USA; [5]JINR, Dubna, Russia; [6]U Mainz, Germany; [7]JAEA, Tokai-mura, Japan; [8]IMP, Lanzhou, China; [9]ITE, Warsaw, Poland

The studies of complete fusion reactions leading to production of superheavy elements (SHE) with $Z \geq 108$ is extremely difficult due to very low production cross sections. Excitation function measurements of evaporation residues from a fusion reaction together with measurements of the fusion – fission cross section provide important experimental information for understanding the process of compound nucleus (CN) formation and its survival in the competition between fission and neutron evaporation. In this work, we report excitation function measurements of the reaction ^{26}Mg + ^{248}Cm leading to element 108, hassium.

Hassium nuclei were produced in the reaction ^{248}Cm(^{26}Mg, x*n*)$^{274-x}$Hs at the linear accelerator UNILAC at GSI, where five beam energies were applied in two experimental campaigns. During the first run [1], two beam energies were applied – 145 and 136 MeV in the middle of the target (E^* = 49 and 40 MeV). These correspond to the calculated maxima [2] of the cross sections for the 5*n* and 4*n* evaporation channel, respectively. In the 4*n* evaporation channel the doubly magic nucleus ^{270}Hs has been produced in the 4*n* evaporation channel for the first time. The same irradiation setup and the same efficient on-line chemical separation and detection system COMPACT has been used in a 2nd run to isolate Hs-isotopes [3]. Three additional beam energies were investigated – 150, 140, and 130 MeV in the middle of the target (E^* = 53, 44, and 35 MeV). In total 26 decay chains from three different Hs isotopes were observed: ^{269}Hs, ^{270}Hs, and ^{271}Hs, produced via 5*n*, 4*n* and 3*n*, respectively [1,3]. Beam integrals and the number of Hs nuclei observed at the five investigated beam energies are presented in Table 1.

Table 1. Irradiation conditions and number of detected Hs decay chains produced in the complete fusion reaction ^{248}Cm(^{26}Mg, x*n*)$^{274-x}$Hs.

E_{Lab}, *MeV*	*Irradiation time, h*	*Beam integral particles,*	*3n* ^{271}*Hs*	*4n* ^{270}*Hs*	*5n* ^{269}*Hs*
130	91	$1.71 \cdot 10^{18}$	0	0	3
136	120	$2.02 \cdot 10^{18}$	2	4	1
140	158	$2.55 \cdot 10^{18}$	1	2	3
145	139	$1.46 \cdot 10^{18}$	0	1	7
150	91	$1.43 \cdot 10^{18}$	0	0	2

Based on the assignment of these chains, the cross sections for the 3*n*, 4*n*, and 5*n* evaporation channels of the reaction ^{248}Cm(^{26}Mg, x*n*)$^{274-x}$Hs were evaluated. Figure 1 shows the measured cross sections together with results from HIVAP [2] calculations. The most likely attribution was used for two chains where no unambiguous attribution of the decay chains was possible. The cross section values varied within the error limits when an alternative attribution was applied. Decay losses during transport to the detection system (about 3 s), were not considered in the cross section calculations.

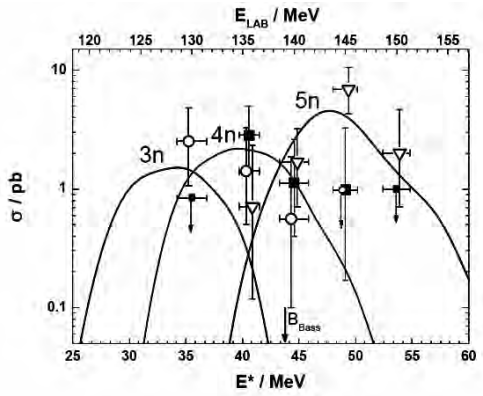

Figure 1: Comparison of production cross sections measured for the reaction ^{248}Cm(^{26}Mg,5-3*n*)$^{269-271}$Hs (symbols) along with excitation functions calculated with HIVAP (lines) [2]. Error bars represent 68% confidence intervals.

Strikingly high cross sections are observed for the 3*n* channel at energies well below the Bass fusion barrier. This indicates that most probably the fusion barrier for favourable collision of deformed nuclei is lower than the conventionally used "Bass barrier" [4] and that multi-dimensional fusion models [5] need to be applied. The observation of the 3*n* channel with cross sections at the same level as the 4*n* and 5*n* channel in the hot fusion reaction ^{26}Mg+^{248}Cm indicates the possible discovery of new neutron-rich transactinide nuclei using relatively light heavy-ion beams of the most neutron-rich stable isotopes and actinide targets.

References

[1] J. Dvorak *et al*., Phys. Rev. Lett. **97**, 242501 (2006).
[2] W. Reisdorf and M. Schädel, Z. Phys. A 343, 47 (1992).
[3] J. Dvorak *et al*., GSI Sci. Rep. 2007, this issue.
[4] R. Bass, Nucl. Phys. A 231, 45 (1974).
[5] K. Nishio *et al*., Phys. Rev. Lett. 93 162701 (2004).

* Work supported by BMBF (06MT247I)

First successful chemistry-experiment behind TASCA –Electrodeposition of Os*

J. Even[1,2,#], W. Brüchle[3], R.A. Buda[1], Ch.E. Düllmann[3], K. Eberhardt[1], E. Jäger[3], H. Jungclas[2], J.V. Kratz[1], J. Khuyagbaatar[3], D. Liebe[1], M. Mendel[1], M. Schädel[3], B. Schausten[3], E. Schimpf[3], A. Semchenkov[3,4], A. Türler[4], V. Vicente Vilas[1], N. Wiehl[1], T. Wunderlich[1], A. Yakushev[4]

[1]Institut für Kernchemie, Johannes-Gutenberg-Universität Mainz, Germany; [2]Fachbereich Chemie, Philipps-Universität Marburg, Germany; [3]GSI, Darmstadt, Germany, [4]Institut für Radiochemie, Technische Universität München, Germany

Underpotential deposition has been shown by Hummrich [1] to be a suitable method for studying the chemical behaviour of the transactinides. For such investigations, the nuclide should have a half-life of at least 10 s. Thus, ^{270}Hs ($T_{1/2}$~22 s [2]) is a good candidate for electrochemical experiments. This report describes the first electrodeposition of short-lived isotopes of osmium, the lighter homologous element of hassium.

Os was produced in the reaction ^{nat}Ce(^{40}Ar,xn). The first experiments took place in cave X1 without preseparation. The reaction products were transported via a He/KCl-jet from the recoil chamber, which was directly behind the target, to a direct catch (DC) apparatus and to the Automated Liquid Online Heavy Element Apparatus (ALOHA). DC samples were collected on glass fibre filters which were measured by γ-spectroscopy. No γ-lines of Os isotopes were visible in the spectra due to the high background of transfer products (see figure 1, top), which clearly demonstrates the need for a physical preseparation [3] for such chemistry experiments. Behind TASCA [4], ^{177}Os and ^{176}Os were seen as the main products (see figure 1, bottom).

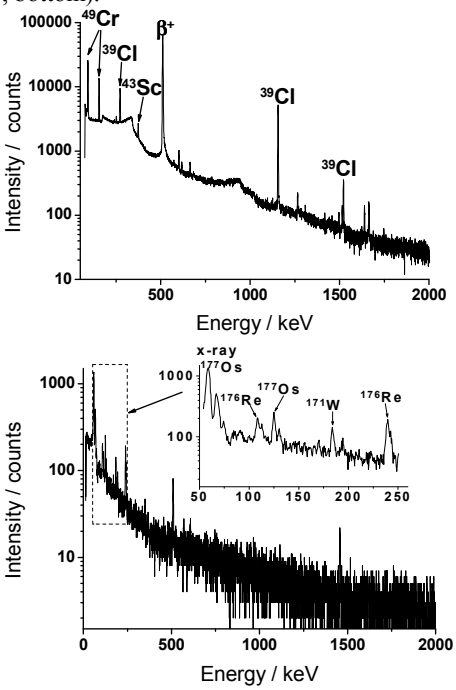

Figure 1: Comparison of the γ-spectra of a sample produced at X1 (top) and at TASCA (bottom).

* Work supported by BMBF (06MZ223I) and GSI-F&E (MZJVKR)
# evenj@uni-mainz.de

For the electrochemical studies, the KCl aerosol particles were transported from the HTM-RTC [5] to the radiochemistry laboratory and were deposited on a Ta plate in ALOHA [1]. After 2 min collection time, the sample was dissolved and flushed into the electrolytic cell with 1 ml 0.1 M HCl delivered by a syringe pump. After running the electrolysis for 2 min, the electrodes were measured with a γ detector. The electrolysis was repeated at various potentials vs. an Ag/AgCl reference electrode. Measurements with different electrode materials (Pd, Ni, and palladinated Ni) were performed. The data were analysed according to [6] as shown in figure 2. The $E_{50\%}$-values, i.e., the potential, at which a deposition yield of 50% was observed, were +81 mV for Pd, +67 mV for palladinated Ni, and +10 mV for Ni, with uncertainties of ±50 mV.

To gain information about the deposition kinetics, the electrode potential was kept constant at -800 mV vs. an Ag/AgCl electrode and the electrolysis duration were varied. At room temperature and non-optimal stirring conditions, half of the osmium was deposited on Pd electrodes within (48±10) s and on Ni electrodes within (54±10) s.

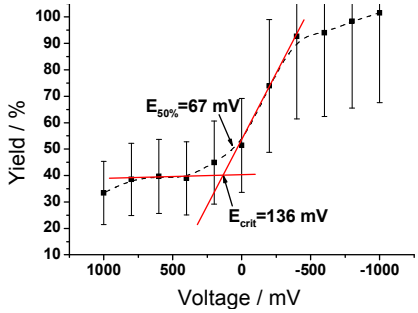

Figure 2: The critical potential on a palladinated Ni-electrode (the dashed line is drawn to guide the eye).

In another experiment with higher beam energy α-decaying ^{172,173}Os were produced and deposited on the Pd electrodes. Due to the small α-branch and the short half-lives (~20 s), only a few counts were detected. It could be shown, however, that it is possible to detect such short-lived nuclides by α spectrometry with an automated electrolytic cell after preseparation with TASCA.

References

[1] H. Hummrich, Doctoral thesis, U. Mainz, 2006.
[2] J. Dvorak et al., Phys. Rev. Lett. **97** (2006) 242501.
[3] Ch.E. Düllmann, Eur. Phys. J. D **45** (2007) 75.
[4] M. Schädel et al., this report.
[5] Ch.E. Düllmann et al., GSI Sci. Rep. 2006, p. 146.
[6] F. Joliot, J. Chim. Phys. **27**, 119 (1930).

Adsorption Behaviour of HsO_4

A. Yakushev[1], J. Dvorak[1], Z. Dvorakova[1], R. Krücken[1], F. Nebel[1], R. Perego[1], R. Schuber[1], A. Semchenkov[1, 2], A. Türler[1], B. Wierczinski[1], W. Brüchle[2], Ch. E. Düllmann[2, 3, 4], E. Jäger[2], V. Pershina[2], M. Schädel[2], B. Schausten[2], E. Schimpf[2], M. Chelnokov[5], V. Gorshkov[5], A. Kuznetsov[5], A. Yeremin[5], K. Eberhardt[6], P. Thörle[6], Y. Nagame[7], K. Nishio[7], Z. Qin[2, 8], and M. Wegrzecki[9]

[1]TU Munich, Garching, Germany; [2]GSI, Darmstadt, Germany; [3]LBNL, Berkeley, CA, USA; [4]UC, Berkeley, CA, USA; [5]JINR, Dubna, Russia; [6]U Mainz, Germany; [7]JAEA, Tokai-mura, Japan; [8]IMP, Lanzhou, China; [9]ITE, Warsaw, Poland

Element 108, hassium, has been chemically identified for the first time by Ch. E. Düllmann *et al.* as a member of group 8 of the periodic table. A lower volatility of HsO_4 ($-\Delta H_{ads}$ = 46 ± 2 kJ/mol) compared to OsO_4 ($-\Delta H_{ads}$ = 39 ± 1 kJ/mol) has been observed [1]. Both extrapolations of ΔH_{ads} from RuO_4 and OsO_4 [2] and relativistic quantum chemical calculations with the use of the physisorption model [3,4] have shown that adsorption of HsO_4 on inert surfaces should almost be equal to that of OsO_4. The experimentally measured values are in disagreement, though not large, of only 6-7 kJ/mol.

Here we report results of two experiments aimed at synthesizing of new Hs isotopes performed recently at GSI. Two new Hs isotopes, $^{270, 271}$Hs and their daughters were successfully synthesized in the 4n and 3n evaporation channel, respectively, of the complete fusion reaction ^{26}Mg(^{248}Cm, xn)$^{274\text{-}xn}$Hs [5,6]. Hs atoms were separated by chemical means as HsO_4 and detected using the new detector setup COMPACT [5]. Products of the nuclear reactions recoiled from the target and were thermalized in a carrier gas (He/O_2 mixture with 10% O_2, 1.5 or 1.8 l/min) at 1.1 bar in the recoil chamber (RC) heated to 400°C. Oxidation started presumably in the RC and was completed on a quartz wool plug at 650°C. This plug also served as a filter for aerosol particles and non-volatile products. The separation factor from non-volatile species was >10^6. Species volatile at room temperature like HsO_4, OsO_4, At, or Rn were transported by the gas flow through a 8-m long PTFE™ capillary to the detection system. Two panels made from Invar™ with 32 PIPS diodes on each panel were combined into a gas tight channel with a narrow gap of 0.5 mm. The exit end of the detector was cooled to –160°C, whereas the entrance was kept at room temperature. The active surface of the diodes was covered with a thin layer of gold (first run) or aluminium (second run). The nearly 4π detection geometry yielded a detection efficiency of more than 80%. The distribution of 26 detected Hs chains along the detector is shown in Fig. 1 in comparison with the deposition peak of $^{172,173}OsO_4$. Using a Monte Carlo model of mobile adsorption [7] the adsorption enthalpy values have been evaluated as $-\Delta H_{ads}(HsO_4)$ = 51 ± 5 kJ/mol and $-\Delta H_{ads}$ (OsO_4) = 42 ± 2 kJ/mol, respectively. The $-\Delta H_{ads}(HsO_4)$ is slightly higher than observed in [1] and the distribution of the Hs events is rather wide. This fact can be explained by the higher gas flow velocity in the detector channel and the gently sloping temperature gradient in the first half of the detector.

* Work supported by BMBF (06MT247I)

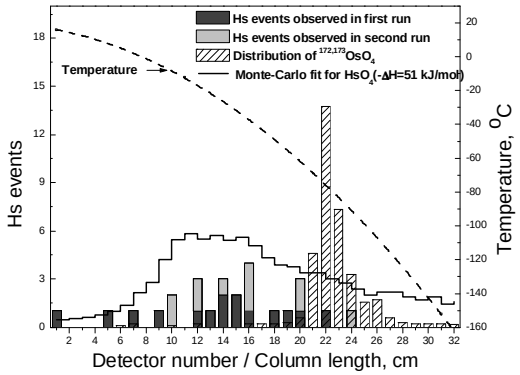

Fig.1. Distribution of HsO_4 and OsO_4 along the detector.

The calculation of the adsorption energy of the Van der Waals interaction of HsO_4 with a surface is sensitive to many parameters. Some of them, such as the ionization potential or the polarizability, can be obtained from accurate electronic structure calculations [3,4]. But it is very difficult to calculate another important parameter – the distance between a molecule and a surface. We propose to use for this parameter a half of the distance between atoms or molecules in molecular crystals. Using these distances in the calculations, the experimental values for adsorption and sublimation enthalpies of noble gases and non-polar molecules, like CH_4, CF_4, SF_6, or RuO_4 and OsO_4 are well reproduced. The intermolecular distance in tetroxide crystals correlates with the bond length between metal and oxygen atoms, which can be calculated theoretically for HsO_4.

Thus, we confirm here an observed earlier lower volatility of HsO_4 compared to OsO_4. This disagreement with the theory caused performance of the new calculations at a higher level of accuracy [8].

References

[1] Ch. E. Düllmann *et al.*, Nature, 418 (2002) 859.
[2] Ch. E. Düllmann *et al.*, J. Phys. Chem. B 106 (2002) 6679.
[3] V. Pershina *et al.*, J. Chem. Phys. 115 (2001) 792.
[4] V. Pershina *et al.*, J. Chem. Phys. 122 (2005) 124301.
[5] J. Dvorak *et al*,. Phys. Rev. Lett. 97, 242501 (2006).
[6] J. Dvorak *et al.*, GSI Sci. Rep. 2007, this issue.
[7] I. Zvara, Radiochim. Acta **38**, 95 (1985).
[8] V. Pershina and J. Anton, GSI Sci. Rep. 2007, this issue

Status of the TASCA Commissioning Program*

M. Schädel[1,#], D. Ackermann[1], W. Brüchle[1], Ch.E. Düllmann[1], J. Dvorak[2], K. Eberhardt[3], J. Even[3], A. Gorshkov[2], R. Gräger[2], K.E. Gregorich[4], F.P. Heßberger[1], A. Hübner[1], E. Jäger[1], J. Khuyagbaatar[1], B. Kindler[1], J.V. Kratz[3], D. Liebe[3], B. Lommel[1], J.P. Omtvedt[5], K. Opel[5], A. Sabelnikov[5], F. Samadani[5], B. Schausten[1], R. Schuber[2], E. Schimpf[1], A. Semchenkov[1,2,5], J. Steiner[1], J. Szerypo[6], A. Türler[2], and A. Yakushev[2] for the TASCA Collaboration

[1]GSI, Darmstadt, Germany; [2]Technical University München, Garching, Germany; [3]University of Mainz, Mainz, Germany; [4]LBNL, Berkeley, CA, U.S.A.; [5]University of Oslo, Oslo, Norway; [6]LMU München, Garching, Germany

The **T**rans**A**ctinide **S**eparator and **C**hemistry **A**pparatus, **TASCA**, project [1] is focusing on the separation and investigation of neutron-rich transactinide nuclides produced in actinide target based reactions. The envisioned research program includes both chemical investigations of transactinide or superheavy elements after preseparation with the gas-filled separator and physics motivated nuclear structure and nuclear reaction studies.

The central device of TASCA is a gas-filled separator in a DQQ configuration. It can be operated in the "High Transmission Mode" (HTM, DQ_hQ_v) and in the "Small Image Mode" (SIM, DQ_vQ_h); see Refs. [1-4] for more details. The separator was installed at the UNILAC beam line X8 and, after having all crucial parts of the control system [5] running, an extensive commissioning program was carried out in 2007. This report briefly summarizes the nuclear reactions applied and the most important parameters studied. A few examples are discussed in a very exemplary way. In addition, recent target developments and the progress in the coupling of chemistry set-ups will be outlined. The first chemical study behind TASCA is described in a separate contribution [6].

All nuclear reactions applied are listed in Table 1 together with the mode of TASCA operation (HTM=H, SIM=S) and the separator gas. Also indicated are experiments aimed to test or apply a recoil transfer chamber (RTC) in addition to measurements performed with a focal plane detector (FPD). As the standard FPD we used a (8x3.6) cm^2 large position-sensitive 16-strip silicon detector. Some experiments were devoted to test prototype double-sided silicon strip detectors (DSSSD) which are planned to be used in future experiments with superheavy elements (SHE).

To understand TASCA as a separator and to build up a solid data base providing good predictive power concerning separator operation for future SHE experiments, we investigated the following most important parameters: (i) the magnetic rigidity of reaction products between Z=76, Os, and Z=102, No, produced at different recoil velocities, and the corresponding best settings of the dipole magnet, (ii) the quadrupole focusing, which is especially relevant for the SIM, (iii) the target thickness dependence of the separator transmission - strongly depending on the asymmetry of the nuclear reaction -, and (iv) the optimum gas pressure with respect to focusing and to transmission - being quite different in the HTM and in the SIM. The analysis of a huge amount of data from these experiments is in progress, and it is important to realize that most of the above mentioned parameters influence each other.

Table 1: Nuclear reactions applied in TASCA commissioning experiments; see text for details.

Beam	Target	Product	Mode	Gas	RTC
^{22}Ne	^{nat}Ta	$^{198m-199}$Bi	H + S	He	
	^{179}Au	^{215}Ac	H + S	He	
	^{238}U	^{255}No	H + S	He	
^{30}Si	no	^{30}Si	H + S	Vac	
	^{181}Ta	$^{205-206}$Fr	H	He	
^{40}Ar	^{nat}Ce	^{173,175}Os	H	He	yes
	^{144}Sm	$^{180-182}$Hg	H + S	He	yes
	^{nat}Gd, ^{152}Gd	$^{194-196}$Pb, ^{188}Pb	H + S	He	yes
	^{nat}Lu	^{210}Ac	H + S	He, N_2	
	^{208}Pb	^{245}Fm	H + S	He	yes
	^{232}Th, ^{238}U	targettest, background	H	He	
^{48}Ca	^{144}Sm	^{188}Pb	H + S	He	
	^{206}Pb	^{252}No	H + S	He	
	^{208}Pb	^{254}No	H	He, H_2	
^{54}Cr	^{nat}Gd	$^{209-210}$Ra	H + S		

Always as a first step, the best dipole setting was found in HTM by centring the product distribution with a typical width of ≈ 6 cm on the FPD. A magnetic rigidity range from 1.5 to 2.2 Tm was covered in those experiments. The quadrupole focusing was found to be insensitive to small quadrupole current changes in the HTM while it reacts very sensitively in the SIM. Optimized SIM settings were determined to obtain maximum rates and narrow distributions of ≈ 1.5 cm FWHM.

The target thickness dependence of the transmission was extensively studied in the reactions ^{22}Ne + ^{197}Au (55, 130, 255, 580 µg/cm^2) and ^{40}Ar + ^{144}Sm (75, 190, 380, 930 µg/cm^2) in both modes. A comparison of these data with model calculations [7] will allow selecting an optimum target thickness with the highest product rate for all the envisioned nuclear reactions.

Many experiments were devoted to find the optimum He pressure and to determine the response to pressure changes. For this we checked the spatial distribution and the total rate of the products in the FPD. While a pressure of about 1 mbar is generally best in the HTM, a signifi-

* Work supported by BMBF (06MT247I, 06MT248, 06MZ223I) and GSI-F&E (MT/TÜR, MZJVKR)
# m.schaedel@gsi.de

cantly lower pressure in the 0.2 to 0.5 mbar range gives optimum results in the SIM. A more detailed investigation of the pressure dependence is under way.

One of the most interesting but least understood parameter in the operation of gas-filled separators is the gas filling. In addition to He as our standard gas, we did first test experiments with H_2, N_2, and mixtures of He and N_2. In the ^{40}Ar + ^{nat}Lu reaction we probed the influence of small amounts of N_2 in He on the magnetic rigidity and tested the pressure dependence in pure N_2. From the ^{48}Ca + ^{208}Pb reaction clean α-spectra of ^{254}No and its daughter ^{250}Fm were measured in the HTM with He and H_2 fillings. Figure 1 shows an example obtained with 1.5 mbar H_2.

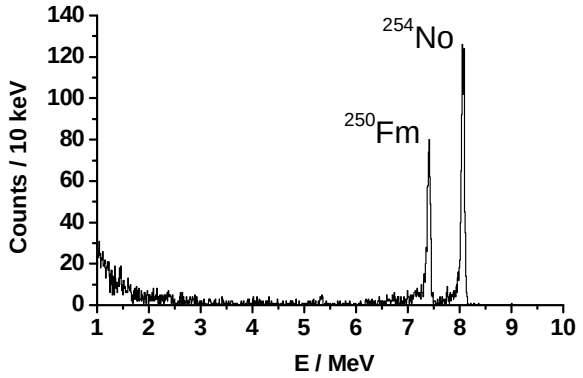

Figure 1: α-spectrum of ^{254}No separated in a 1.5-mbar H_2 gas filling of TASCA. ^{250}Fm is the daughter nucleus.

The ^{22}Ne(^{181}Ta,xn)^{198m,199}Bi reaction was used to check the calculated transmission [7] in the HTM and in the SIM. ^{198m,199}Bi were collected in Al catcher foils directly behind the target (used as the 100% reference value) and in the focal plane. Subsequent γ-ray spectroscopic measurements of these foils allowed determining the transmission and, from a measurement of segments, the spatial product distribution in the focal plane. Very good agreement was found between theoretically calculated transmissions and distributions and the measured ones.

Target development and testing with ^{40}Ar beams of up to 2 μA(particle) continued and concentrated on metallic Th and U targets on 2 μm Ti backings. In addition, large varieties of ^{144}Sm, ^{179}Au and ^{206,208}Pb targets were prepared and used for intense parameter studies at TASCA. Preparations towards new transuranium targets were concentrating on ^{244}Pu. In this ongoing program, considerable progress has been achieved recently.

Commissioning experiments for the RTCs [8], which were built for both two ion-optical modes, focused on finding best conditions for transporting preseparated nuclides to sites where chemistry experiments are envisaged to take place, i.e., a position inside X8 as well as in the nearby radiochemistry laboratory. Suitable nuclides were produced with ^{40}Ar beams, e.g., α-decaying 25-s ^{188}Pb and 4-s ^{245}Fm as well as longer-lived Os, Hg, and Pb isotopes that were identified with γ-ray spectroscopy.

Yields of preseparated Pb isotopes, transported with a He/KCl gas-jet to the chemistry laboratory, were measured as a function of parameters like (i) the thickness of degrader foils installed in front of the RTC window, (ii) the RTC depth, (iii) the pressure inside the RTC, and (iv) the gas-flow rate. Maximum yields of about 65% were obtained for transport to the radiochemistry laboratory through a 10-m long PE capillary at He flow rates of 2.5 L/min at a pressure of 1.2 bar in the RTC.

The product range in the He-filled RTC was measured by inserting catcher foils to positions with different distances from the RTC window. The measured ranges in He turned out to be larger than the values predicted by SRIM calculations, even though the energy loss in the Mylar degrader foil and window agrees well with such calculations. This was confirmed in measurements of EVRs in the FPD after passing through degrader foils.

Preseparated ^{188}Pb was measured after transport into ROMA [9]. Clean α-spectra and high yields allowed determining the half-life of (23.4±0.4) s with better precision than the literature value of (24.2±1.0) [10]. Furthermore experiments were performed where ^{245}Fm was transported into ROMA; see Figure 2. They prove that the TASCA-RTC system is ready for experiments with SHE.

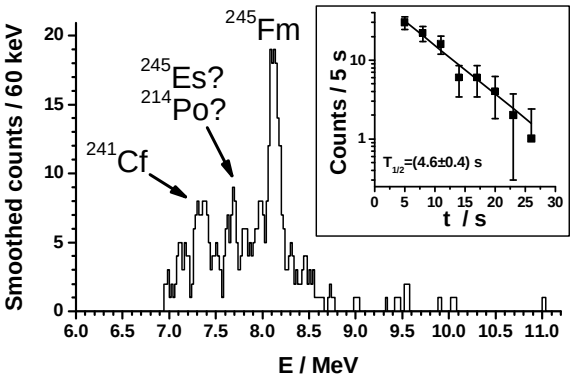

Figure 2: α-spectrum of ^{245}Fm. The insert shows the decay curve for α-particles with 8.05 MeV < E_α < 8.25 MeV.

References

[1] M. Schädel *et al.*, GSI Sci. Rep. 2005, GSI Report 2006-1, 2006, p. 262, and http://www.gsi.de/TASCA
[2] A. Semchenkov *et al.*, GSI Sci. Rep. 2004, GSI Report 2005-1, 2005, p. 332.
[3] M. Schädel, Eur. Phys. J. D 45 (2007) 67.
[4] A. Semchenkov *et al.*, Proceedings EMIS '07, Nucl. Instr. Meth. B, submitted.
[5] E. Jäger *et al.*, GSI Sci. Rep. 2005, GSI Report 2006-1, 2006, p. 263.
[6] J. Even *et al.*, this report.
[7] K.E. Gregorich *et al.*, GSI Sci. Rep. 2006, GSI Report 2007-1, 2007, p. 144.
[8] Ch.E. Düllmann *et al.*, GSI Sci. Rep. 2006, GSI Report 2007-1, 2007, p. 146.
[9] K. Sümmerer *et al.*, GSI Sci. Rep. 1983, GSI Report 84-1, 1984, p. 246.
[10] R.B. Firestone and V.S. Shirley (Eds)., Table of Isotopes, 8th edition, Vol. II

Spin-Polarized 4c-DFT Calculations of the Electronic Structures and Properties of MO_4 (M = Ru, Os, and Hs) and Prediction of Physisorption

V. Pershina[1] and J. Anton[2]
[1]GSI, Darmstadt, Germany; [2]University of Kassel, Kassel, Germany

Volatility of group 8 tetroxides, MO_4 (M = Ru, Os, and Hs) has been a subject of interest of both experimental and theoretical research. Theoretically, very similar electronic structures and properties including volatilities were predicted on the basis of fully relativistic, four-component, density functional theory (4c-DFT) calculations [1,2]. Using a model of physisorption, it was shown that adsorption of HsO_4 on inert surfaces should almost be equal to that of OsO_4. Similar conclusions were obtained using extrapolation in group 8 [3]. Two similar types of experiments have, however, demonstrated that HsO_4 is about 6-7 kJ/mol stronger adsorbed on inert surfaces than OsO_4 [4,5]. In order to understand the reason for this (modest) disagreement, we have undertaken this study at a higher level of theory than before.

Thus, in this work, we have newly calculated the electronic structures of MO_4 (M = Ru, Os, and Hs) using our new version of the 4c-DFT method, which takes into account also magnetic effects [6]. The method implies the solution of the Kohn-Sham equations which in the non-collinear approximation have the form

$$\left\{\hat{t}+V^N+\tilde{V}^H+\frac{\delta E^{xc}[\rho,\vec{m}]}{\delta\rho}-\mu_B\beta\vec{\Sigma}\frac{\delta E^{xc}[\rho,\vec{m}]}{\delta\vec{m}}\right\}\phi_i=\varepsilon_i\phi_i \quad (1)$$

where ρ is electronic and m is magnetization densities. The wavefunctions ϕ are four-component Dirac spinors.

We have also dramatically increased the basis sets, which are now 5p,5d,4f,6s6p,5f for Ru; 6p,6d,5f,7s7p,7d for Os and 7p,7d,6f,8s8p,5g for Hs. These improvements allowed us to reach very high accuracy of the calculated polarizabilities, α, in almost perfect agreement with experiment for RuO_4 and OsO_4 [7] (Table 1). The present calculations have demonstrated a remarkable increase in $\alpha(HsO_4)$ in comparison with the earlier calculations due to a more complete inclusion of correlation effects, as well as improvements in the code.

The geometry (bond lengths, R_e) has been newly optimized in the present calculations. The obtained spectroscopic properties – ionization potentials (IP), α, vibrational frequencies (w_e) and R_e- are given in Table 1. They show very good agreement with the measured values for RuO_4 and OsO_4.

The dispersion interaction energies of the MO_4 molecules with quartz were calculated using the equation [1,2]

$$E(x)=-\frac{3}{16}\left(\frac{\varepsilon-1}{\varepsilon+2}\right)\frac{\alpha_{mol}}{\left(\frac{1}{IP_{slab}}+\frac{1}{IP_{mol}}\right)x^3} \quad (2)$$

Table 1. Calculated IP (in eV), polarizabilities, α (in a.u.), vibrational frequences, w_e (in cm^{-1}), bond lengths, R_e (in a.u.), molecule-surface distances x (in a.u.) and energies of physisorption, $-\Delta H_{ads}$ on quartz (in kJ/mol) for MO_4 (M = Ru, Os, and Hs).

Property	RuO_4	OsO_4	HsO_4	Ref.
IP	12.25	12.35	12.28	calc. [2]
	12.19	12.35	-	exp. [7]
α	58.07	55.28	65.995	this
	58.64	55.13	-	exp. [7]
w_e	1215	1284	1413	this
	-	965	-	exp.
R_e	1.712	1.719	1.779	this
	1.706	1.711	-	exp. [7]
x	2.228	2.23	2.25	this
$-\Delta H_{ads}$	40.23	39	46.5	this
	-	39±1	46±2	exp. [4]

The molecule-surface distances x have been newly estimated (Table 1) using the calculated R_e and assuming that the T_d molecules touch the surface by their facets.

The newly calculated ΔH_{ads} (Table 1) are in perfect agreement with the experimental results [4]. Thus, there is, indeed, a reversal of the trend in group 8 from Os to Hs not only in atomic properties such as IP or α, but also in the interaction energies with the surrounding, which are defined by those properties in a complex way (eq. 2). A reversal of the trend in ΔH_{ads} in group 8 takes its origin from the behaviour of the d-valence atomic orbitals (see Fig. 1 in Ref. [2]).

Thus, both experiments [4,5] and theory have finally agreed on the reversal of the trend in ΔH_{ads} in group 8, which could not be predicted on the basis of the extrapolation in the group. This remarkable example shows that in the case of weak interactions (van der Waals), very accurate calculations with electron correlation at the best level should be performed for the heaviest elements.

References

[1] V. Pershina *et al.* J. Chem. Phys. 115 (2001) 792.
[2] V. Pershina *et al.* J. Chem. Phys. 122 (2005) 124301.
[3] Ch. E. Düllmann *et al.* J. Phys. Chem. B 106 (2002) 6679.
[4] Ch. E. Düllmann *et al.* Nature, 418 (2002) 859 .
[5] A. Yakushev *et al.* GSI Annual Report 2007, this issue.
[6] J. Anton *et al.* Phys. Rev. A 69 (2004) 012505.
[7] CRC Handbook of Chemistry and Physics, 86th edition, ed. D. R. Lide (2005).

Prediction of the Adsorption Behaviour of Pb and Element 114 on Inert Surfaces from *ab initio* Dirac-Coulomb Atomic Calculations

V. Pershina[1], A. Borschevsky[2], E. Eliav[2], and U. Kaldor[2]
[1]GSI, Darmstadt, Germany; [2]Tel Aviv University, Israel

For the chemical identification of the heaviest elements, like 112 and 114, which are of current interest, predictions of their adsorption behaviour on various surfaces used in the experiments are essential. Recently, we have predicted adsorption of element 114 and its homolog Pb on metal surfaces on the basis of the fully relativistic density functional theory calculations of intermetallic compounds [1]. Inert surfaces such as quartz or Teflon can also be used, as well as ice can be formed in the chromatography column at very low temperatures. Information about the interaction of the heaviest elements with inert surfaces is also valuable for designing their transport from the target to the experimental set up. Thus, in this work, we predict the adsorption behaviour of element 114 and its homolog Pb on inert surfaces on the basis of very accurate results of *ab initio* calculations of their atomic properties.

The electronic structure calculations were performed using the DIRAC package [2]. In the Dirac-Coulomb (DC) *ab initio* method, the many-electron relativistic Dirac-Coulomb Hamiltonian

$$H_{DC} = \sum_i h_D + \sum_{i<j} 1/r_{ij} \qquad (1)$$

is employed, where

$$h_D = c\vec{\alpha}\cdot\vec{p} + \beta c^2 + V_{nuc}\,. \qquad (2)$$

The atomic orbitals are four-component spinors

$$\phi_{nk} = \begin{pmatrix} P_{nk}(r) \\ Q_{nk}(r) \end{pmatrix}, \qquad (3)$$

where $P_{nk}(r)$ and $Q_{nk}(r)$ are the large and small component, respectively. The Faegri uncontracted 26s24p18d13f5g2h basis set was used for both elements [3]. Electron correlation was taken into account at various levels of theory including the highest, the Coupled Cluster Single Double (Triple) excitations, CCSD(T), for which the current results are presented.

The calculations of polarizability (α) were performed with the use of the finite field method. The DC CCSD(T) results for α are given in Table 1 along with the ionization potentials (IP) of Pb and element 114 calculated at best using the Dirac-Coulomb-Breit Fock-Space CC (DCB FSCC) method [4]. The van der Walls radii (R_{vdW}) were determined from a linear correlation with $R_{max}(np_{1/2})$-atomic orbitals of the group 14 elements. The adsorption enthalpies, ΔH_{ads}, were calculated using a model of physisorption given by eq. (8) of Ref. [5].

Table 1. Atomic properties of Pb and element 114: ionization potentials, IP (in eV), polarizabilities, α (in a.u.), van der Walls radii, R_{vdW} (in a.u.) and energies of physisorption, $-\Delta H_{ads}$ on quartz (q), ice (i) and Teflon (T) (in kJ/mol).

Property	Pb	Meth.	Ref.	114	Meth.	Ref.
IP	7.349	DCB	[4]	8.539	DCB	[4]
	7.417	exp.	[6]			
α	46.96	DC	this	30.59	DC	this
	45.89	exp.	[6]			
R_{vdW}	4.06	corr.	this	3.94	corr.	this
	4.16	exp.	[6]			
$-\Delta H_{ads}$ (q)	27.34	calc.	this	20.97	calc.	this
$-\Delta H_{ads}$ (i)	26.29	calc.	this	20.20	calc.	this
$-\Delta H_{ads}$ (T)	13.65	calc.	this	10.41	calc.	this
	13.0	exp.				

The obtained ΔH_{ads} on quartz and Teflon for all group 14 elements are shown in Fig. 1 revealing a reversal of the trend from Sn on. The very low ΔH_{ads}(114) on inert materials guarantees its transport to the chemistry set up.

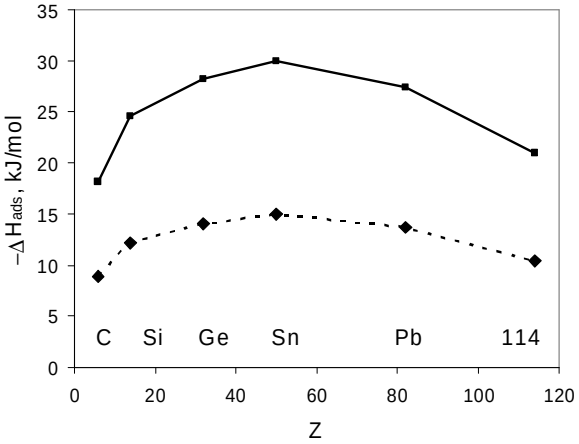

Fig. 1. Calculated dispersion interaction energies (enthalpies of adsorption, $-\Delta H_{ads}$) of group 14 elements with quartz (solid line) and Teflon (dashed line).

References

[1] V. Pershina, J. Anton, and B. Fricke, J. Chem. Phys. 127, (2007) 134310.
[2] DIRAC 04, written by H. J. Ja. Jensen *et al.* (2004).
[3] K. Faegri, Theor. Chim. Acta 105 (2001) 252 .
[4] A. Landau *et al*. J. Chem. Phys. 114 (2001) 2977.
[5] V. Pershina *et al*. J. Chem. Phys. 122 (2005) 124301.
[6] CRC Handbook of Chemistry and Physics, 86th edition, ed. D. R. Lide (2005).

Fully Relativistic *ab initio* Dirac-Coulomb Calculations of Atomic Properties of Rn and Element 118

A. Borschevsky[1], E. Eliav[1], U. Kaldor[1], and V. Pershina[2]
[1]Tel Aviv University, Israel; [2]GSI, Darmstadt, Germany

Experiments on the production of elements 112-116 in Dubna, Russia, have proven the existence of the enhanced stability of their neutron-rich isotopes. Furthermore, the existence of element 118 has been demonstrated using the ^{48}Ca beam and the ^{249}Cf target [1]. The produced ^{294}118 isotope has half-life $T_\alpha=0.89^{+1.07}_{-0.31}$ ms in agreement with the theoretical predictions and decays into ^{286}114 or ^{282}112, which undergo spontaneous fission,.

Chemical identification of element 118 is a matter of the near future. Predictions of its chemical properties, especially those important for gas-phase chromatography experiments [2] are, therefore, needed. Very accurate calculations can nowadays be performed using fully relativistic methods and algorithms. Thus, in this work we predict atomic properties of element 118 and its homolog Rn on the basis of *ab initio* Dirac-Coulomb (DC) calculations using the DIRAC package [3]. In the DC *ab initio* method, the many-electron relativistic Dirac-Coulomb Hamiltonian

$$H_{DC} = \sum_i h_D + \sum_{i<j} 1/r_{ij} \qquad (1)$$

is employed, where

$$h_D = c\vec{\alpha}\cdot\vec{p} + \beta c^2 + V_{nuc}\,. \qquad (2)$$

The atomic orbitals are four-component spinors

$$\phi_{nk} = \begin{pmatrix} P_{nk}(r) \\ Q_{nk}(r) \end{pmatrix}, \qquad (3)$$

where $P_{nk}(r)$ and $Q_{nk}(r)$ are large and small component, respectively. The Faegri uncontracted 26s24p18d13f5g2h basis set was used for Rn and element 118 [4]. The electron correlation was taken into account at various levels of theory - Moller-Plesset (MP2) and Coupled Cluster Single Double (Triple) excitations [CCSD(T)]. The Hartree-Fock (HF) values were also obtained for comparison in order to elucidate the influence of correlation.

The calculations of polarizability (α) were performed with the use of the finite field method. The strengths of the field were chosen as 0.0001, 0.001 and 0.01 a.u. The results are summarized in Table 1. The obtained DC CCSD(T) values are in very good agreement with experiment for Rn [5] and much better than those calculated in Ref. [6] using the MOLFDIR code. The latter values are not accurate due to the small basis sets used. The α(118) is larger than α of the other gases due to the relativistic expansion of the outer $7p_{3/2}$ atomic orbitals (AOs).

Table I. Polarizabilities α (in a.u.) for Rn and element 118 calculated at different levels of correlation.

Atom	α				Ref.
	HF	MP2	CCSD	CCSD(T)	
Rn	34.99	34.96	34.78	35.04	present
	29.22	28.48	28.61	28.61	calc. [6]
	-	-	-	35.766	exp. [5]
118	50.01	44.45	46.64	46.33	present
	54.46	49.47	52.50	52.43	calc. [6]

We also give here estimates of atomic, or van der Walls radii (R_{vdW}) of element 118. They were determined using a correlation between the maximum of the radial charge density of the outer valence $np_{3/2}$ AOs [7] and known R_{vdW} (Fig. 1). The obtained $R_{vdW}(118)$ is larger than R_{vdW} of the other gases due to the same reason an that for α.

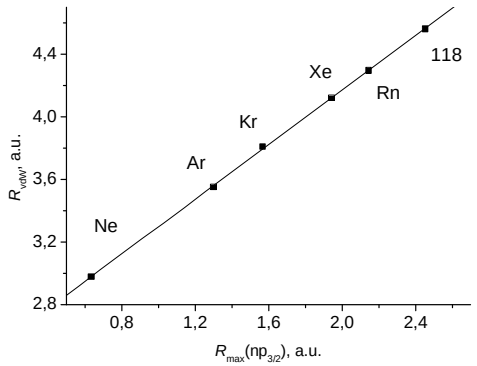

Fig. 1. Correlation between $R_{max}(np_{3/2})$ and R_{vdW} for the rare gases. The obtained value for $R_{vdW}(118)$ = 4.55 a.u.

The calculated properties can be used for further predictions of adsorption behaviour of these elements on various surfaces.

References

[1] Yu. Ts. Oganessia *et al.* Phys. Rev. C 74 (2006) 044602.
[2] H. W. Gäggeler, A. Türler, In: Chemistry of Superheavy Elements, ed. M. Schädel, Kluwer, 2003.
[3] DIRAC 04, written by H.J. Ja. Jensen *et al*. (2004).
[4] K. Faegri, Theor. Chim. Acta 105 (2001) 252 .
[5] CRC Handbook of Chemistry and Physics, 86th edition, ed. D. R. Lide (2005).
[6] C. Nash, J. Phys. Chem. 109 (2005) 3493.
[7] J. P. Desclaux, At. Data Nucl Data Tables, 12 (1973) 311.